

Guidance, navigation and control of a powered parafoil aerial vehicle

Vindhya Devalla^{1,*}, Amit Kumar Mondal², A. J. Arun Jeya Prakash¹,
Manish Prateek³ and Om Prakash¹

¹Aerospace Engineering Department,

²Electronics, Instrumentation and Control Engineering Department, and

³Centre for Information Technology, University of Petroleum and Energy Studies, Dehradun 248 007, India

One of the most important issues currently facing the oil and gas industries is the safety and security of pipelines which deliver crude oil from the reservoir to the refineries. Many complications such as waxing, slugging, rusting, theft, etc. obstruct the regular supply of fuel to the refineries. Continuous monitoring of pipelines is a major hurdle because of climatic conditions, length of the pipelines, identification of leakage, etc. Here we showcase an unmanned autonomous powered parachute aerial vehicle designed for monitoring such pipelines, thereby paving a way to solve this problem. The vehicle would follow a planned trajectory for following the pipeline effectively. We present here guidance, navigation and control of a powered parachute aerial vehicle. A nine degree of freedom mathematical model has been presented in detail. Lateral heading and longitudinal altitude hold controller was designed for this purpose. A path planning algorithm verified by actual flight parameters has been designed for following a trajectory using way point navigation.

Keywords: Aerial vehicle, altitude hold, dynamic modelling, heading control, waypoint navigation.

PARAFOIL is entirely made of fabric and is a non-rigid wing. It gets inflated like a parachute when dropped from a height. The wing has a low aspect ratio with an elliptical or a rectangular plan form when inflated. To act as an airfoil, the upper and lower membranes are sewn together with a gap between both. The leading edge is kept open so as to allow the air inside the cells creating air pressure, which maintains the shape of the parafoil as a wing¹. The vents in the ribs allow the air to pass from one cell to another which helps in maintaining uniform air pressure in the wing. To avoid air loss, the fabric is made of non-porous material. Suspension lines are used to connect the parafoil to the 'fly-bar' which is attached to payload (Figure 1).

The course of a powered parafoil is controlled by the pilot, by pulling (or tilting) on either side of the fly-bar (appended to a servo engine) that pulls down a line asso-

ciated with the trailing edge of the canopy. This activity alters the course of the lift making the aircraft turn.

The powered parafoil tends to fly at consistent speed. These systems have pendulum stability and oscillations, because the mass of the airframe suspended fundamentally beneath the canopy. This allows the framework to have a yaw motion rather than roll motion². Lateral control is obtained by the canopy itself and the propulsion system attached to the payload. Addition of propulsion system makes the paraglider an unmanned aerial vehicle³.

This article presents guidance, navigation and control algorithm design for lateral and longitudinal motion both theoretically and practically. Initially, parafoil aerial vehicle (PAV) modelling was done, followed by designing of lateral and longitudinal controllers. The gain values for both controllers were calculated theoretically. After the theoretical gain calculations for lateral and longitudinal controllers, practical algorithms for the guidance law were developed. The guidance laws were followed by attitude stability of PAV. Once PAV's attitude was stabilized, the lateral heading and longitudinal altitude hold controllers were implemented. The gains required for practical testing were then identified by continuous flight tests. Guidance law algorithms were designed to program the on-board controller. The two main algorithms designed for guidance law. Steer to target function and path deviation function were used for autonomous way point navigation of PAV. The flight tests were then conducted to demonstrate way point navigation and are discussed here.

Equation (1) gives the 9 Degrees of Freedom (9 DoF) model. The parafoil payload model is demonstrated as a two-body framework comprising canopy mass, and a payload mass suspended below it using the suspension lines. The guiding arrangement utilized is known as a 'fly-bar'. In this outline, the parafoil is associated with the ends of the fly-bar. This bar can be pulled either side of the aircraft, altering the course of the lift, making the PAV turn. This type of parafoil, payload model uses 9 DoF model⁴ as shown in Figure 2. The model having 9 DoF, with two-body dynamics, consists of three degrees of freedom for rotational motion of the parafoil, three degrees of freedom for the rotational movement of the

*For correspondence. (e-mail: vindhsdevalla@yahoo.com)

payload and three degrees of freedom for translational motion of the parafoil.

The separation between the aerodynamic centre of the canopy and the payload centre of gravity produces a swinging motion. In the 9 DOF model two masses m_b and m_p (mass of the payload and parafoil) are connected at point C . R_b and R_p are two rigid massless links that connect parafoil and payload at joint C . The two bodies are allowed to pivot about C (ref. 5). In this model the spring damper modelling of relative yawing motion in parafoil and payload due to the lines has been utilized. Three reference frames have been used namely parafoil reference frame, body reference frame and the joint C reference frame. Three forces acting on parafoil have been modelled as, aerodynamic force, gravitational force and internal force due to joint C . Similarly, four forces which are acting on the payload are modelled as, aerodynamic



Figure 1. Powered parafoil aerial vehicle.

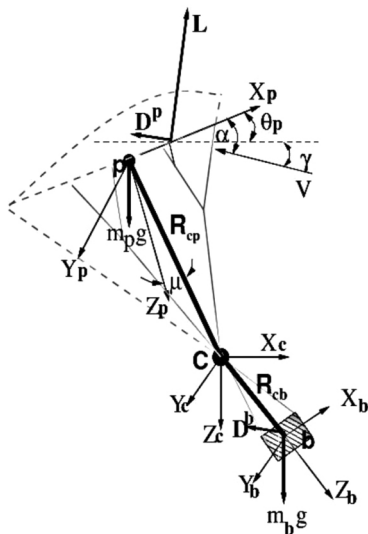


Figure 2. 9 degrees of freedom powered parafoil aerial vehicle.

force, gravitational force, thrust force and internal force due to joint C . Aerodynamic moment is modelled for the parafoil. The rotational spring-damper is modelled as M_c .

Force equations of payload and parafoil model

$$M_b \dot{V}_b + \Omega_b \times M_b V_b = F_b^A + F_b^G + F_b^T - F_b^C, \quad (1)$$

$$F_b^A = \bar{q}_b S_b \begin{Bmatrix} C_{ab} C_D^b \\ 0 \\ S_{ab} C_D^b \end{Bmatrix}, \quad F_b^G = m_b g \begin{Bmatrix} -S\theta_b \\ S\phi_b C\theta_b \\ C\phi_b C\theta_b \end{Bmatrix},$$

$$F_b^C =$$

$$\begin{bmatrix} C\theta_b C\psi_b & C\theta_b S\psi_b & -S\theta_b \\ S\phi_b S\theta_b C\psi_b - C\phi_b S\psi_b & S\phi_b S\theta_b S\psi_b + C\phi_b C\psi_b & S\phi_b C\theta_b \\ S\phi_b S\theta_b C\psi_b + S\phi_b S\psi_b & C\phi_b S\theta_b S\psi_b - S\phi_b C\psi_b & C\phi_b C\theta_b \end{bmatrix}$$

$$\times \begin{Bmatrix} F_{cx} \\ F_{cy} \\ F_{cz} \end{Bmatrix}, \quad (2)$$

$$F_b^T = \begin{Bmatrix} Th \\ 0 \\ 0 \end{Bmatrix},$$

$$(M_p + M_F) \dot{V}_p + \Omega_p \times (M_p + M_F) V_p = F_p^A + F_p^G - F_p^C, \quad (3)$$

$$F_p^A = \bar{q}_p S_p \begin{Bmatrix} C_X \\ C_Y \\ C_Z \end{Bmatrix},$$

$$F_p^G = m_p g \begin{Bmatrix} -S\theta_p \\ S\phi_p C\theta_p \\ C\phi_p C\theta_p \end{Bmatrix},$$

$$F_p^C =$$

$$\begin{bmatrix} C\theta_p C\psi_p & C\theta_p S\psi_p & -S\theta_p \\ S\phi_p S\theta_p C\psi_p - C\phi_p S\psi_p & S\phi_p S\theta_p S\psi_p + C\phi_p C\psi_p & S\phi_p C\theta_p \\ S\phi_p S\theta_p C\psi_p + S\phi_p S\psi_p & C\phi_p S\theta_p S\psi_p - S\phi_p C\psi_p & C\phi_p C\theta_p \end{bmatrix}$$

$$\times \begin{Bmatrix} F_{cx} \\ F_{cy} \\ F_{cz} \end{Bmatrix}. \quad (4)$$

Equations (1) to (4) give the force equations for parafoil and payload.

Moment equations of payload and parafoil model

$$I_b \dot{\Omega}_b + \Omega_b \times I_b \Omega_b = R_{cb} \times F_b^C, \tag{5}$$

$$I_p \dot{\Omega}_p + \Omega_p \times I_p \Omega_p = M_p - R_{cp} \times F_p^C. \tag{6}$$

Kinematic equations

$$\begin{Bmatrix} \dot{x}_c \\ \dot{y}_c \\ \dot{z}_c \end{Bmatrix} = \begin{Bmatrix} u_c \\ v_c \\ w_c \end{Bmatrix}.$$

$$\begin{Bmatrix} \dot{\phi}_b \\ \dot{\theta}_b \\ \dot{\psi}_b \end{Bmatrix} = \begin{bmatrix} 1 & S\phi_b t\theta_b & C\phi_b t\theta_b \\ 0 & C\phi_b & -S\phi_b \\ 0 & \frac{S\phi_b}{C\theta_b} & \frac{C\phi_b}{C\theta_b} \end{bmatrix} \begin{Bmatrix} p_b \\ q_b \\ r_b \end{Bmatrix}.$$

$$\begin{Bmatrix} \dot{\phi}_p \\ \dot{\theta}_p \\ \dot{\psi}_p \end{Bmatrix} = \begin{bmatrix} 1 & S\phi_p t\theta_p & C\phi_p t\theta_p \\ 0 & C\phi_p & -S\phi_p \\ 0 & \frac{S\phi_p}{C\theta_p} & \frac{C\phi_p}{C\theta_p} \end{bmatrix} \begin{Bmatrix} p_p \\ q_p \\ r_p \end{Bmatrix}. \tag{7}$$

Lateral controller design

The controller has a heading tracking function, which receives the target heading angle from the higher level guidance logic and outputs a control signal to reduce the error among measured and target heading⁴. Classical feedback controller is adopted such that the gyroscope output can be used directly.

The servo is modelled by simple first order transfer. The servo transfer function is simply

$$T_{servo} = 14.7 / (S + 14.7). \tag{8}$$

Two gains should be tuned to tune the lateral heading controller, i.e. K and K_f , respectively (Figure 3). The transfer function of PAV is taken to be T_{pav} with input δ_a and output ψ .

The transfer function for minor loop is given by

$$T_{minor} = \frac{T_{servo} T_{pav}}{1 + K_f T_{servo} T_{pav}}. \tag{9}$$

It is determined that $K_f = 2.8$ by considering the root locus of T . The closed loop then becomes the open loop transfer function

$$T_{major} = \frac{K T_{servo} T_{pav}}{1 + (K_f + K) T_{servo} T_{pav}}. \tag{10}$$

It is determined that $K = 1.8$ by considering the root locus of T_{major} .

Longitudinal controller design

The controller has an altitude tracking function, which receives the target altitude from the guidance scheme and outputs throttle signal to minimize the error between the measured and the target altitude⁴. A classical proportional, integral and derivative (PID) controller was implemented (Figure 4).

A throttle control scheme was developed. A PID controller was designed and implemented in the cascade configuration scheme. PID gives the exact signal to be supplied to the motor to eliminate the steady state altitude error. A simple feedback loop has been used to stabilize PAV.

The brushless DC motor is modelled by the first order transfer function, $T_{raise} = 2.2/t$, $t = 1$ sec. The motor transfer function is simply⁶

$$T_{motor} = 2.2 / (S + 2.2). \tag{11}$$

A relationship between thrust and altitude is developed so altitude gained is linearly proportional to the throttle provided. Therefore, the altitude response to the throttle value is given as⁴

$$\dot{Z} = K_{alt} (f_T - f_{T0}), \tag{12}$$

where, f_{T0} is the thrust required for level flight, and K_{alt} is constant. To obtain transfer function two assumptions are made. First we assume that the control thrust signal $f_T = \Delta f_T + \Delta f_{T0}$. The thrust is proportional to the throttle input δ_{th} . The δ_{th} is allowed to vary from 0 to unity. We can model the relationship with simple transfer function

$$T_{alt} = K_{alt} / s. \tag{13}$$

The constant K_{alt} is estimated experimentally by providing step input to the throttle. The motor is capable of providing maximum thrust of 10N. With the experiment, K_{alt} is assumed to be 4.5 m/sec. A PID is designed for the system that consists of T_{pav} , T_{motor} and T_{alt} in series.

PD compensator is the introduced of form⁵

$$T_{PD} = (S + Z_{PD}). \tag{14}$$

The controller zero Z_{PD} is chosen as 7.60. PI compensator is given as

$$T_{PI} = (S + Z_{PI}) / s. \tag{15}$$

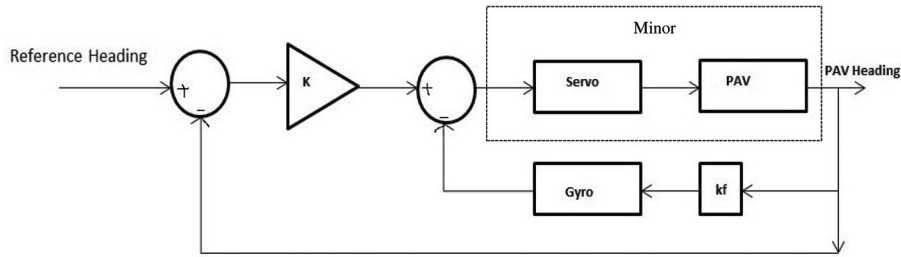


Figure 3. Lateral heading controller.

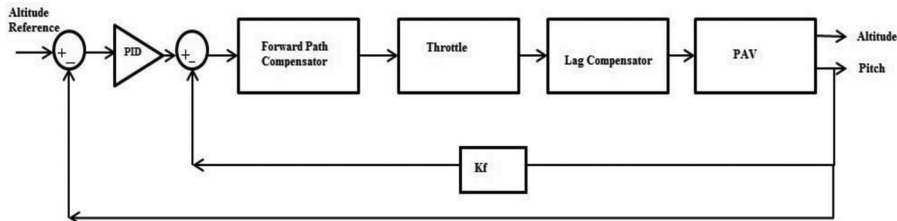


Figure 4. Longitudinal altitude hold controller.

The compensator zero Z_{p1} is arbitrarily chosen as 0.01. The gain is readjusted to 0.0224. The final PID controller is given by

$$T_{PID} = \frac{0.0224(S + 7.60)(S + 0.01)}{S} \quad (16)$$

The proportional derivatives and integrals therefore given by $K_p = 0.1701$, $K_d = 0.0224$, $K_i = 0.0017$ respectively.

Guidance logic

Guidance logic generates heading and altitude signals that will enable the PAV to follow desired path specified by the sequence of points. For autonomous flight, our only concern is to maintain the altitude; hence, the guidance logic is only concerned with the heading angle of the vehicle in the horizontal plane. A simple scheme was implemented (Figure 5), which shows the guidance logic and the specified distance to generate heading angle that will direct PAV back to the path between the waypoints. Before implementing the lateral and longitudinal controller, an attitude stabilizer was implemented to stabilize the PAV. The gains derived out of the guidance law were directly used in flight test programming commands.

Attitude stabilizer

The attitude of PAV is controlled by a nested PI → PID loop. Tuning the inward PID circle is vital to great stable flight. The outer PI loop is less delicate and impacts the most part the style of flying sought (quick or moderate). The inner PID loop takes a gander at the sought rate of precise turn and thinks about that to the crude gyro yield.

The difference is fed back into the PID controller and sent to the motor to correct the rotation. This is important for both rate mode, stabilize mode, and all other modes. It is also the most critical gain to adjust for PAV. The outer PI loop produces the craved rate of precise turn. The contribution for this circle can either be given by the client with stick development of the remote control, or the stabilizer, which tries to accomplish a particular angle.

- STABILITY_P (Figure 6) is 1.3 or 1.3° every second turn for each 1° of error. In the event of more or less speed of rotation based on user input, adjust this value.
- STABILITY_I is 0.1, used to overcome unevenness in the PAV. In the event that the PAV is not symmetrical this term will convey the PAV to level. The higher the number the quicker the PAV will adjust. Low numbers can have adverse impacts by bringing about a moderate swaying measured in seconds.
- RATE_P is the proportional response and the default is 0.2. The PAV will shift a lot contingent upon the weight and thrust of the motor.

PI control for loiter and navigation

For loiter and navigation, the angle between the PAV velocity vector and the next waypoint is calculated (η) called as heading deviation angle. The algorithm starts with selecting a reference waypoint $K + 1$ (Figure 5). The reference point is at a distance L (look-ahead distance) to the current location. Heading deviation angle η is used to calculate the lateral acceleration. Given as $acc = 2(V^2/L)\sin\eta$. The direction of acceleration relies on the indication of the angle between the L line portion and the vehicle speed vector (Figure 5).

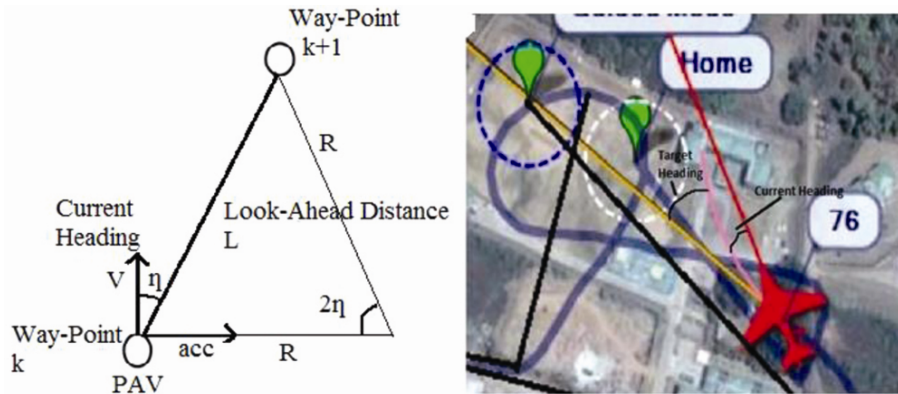


Figure 5. Guidance law.

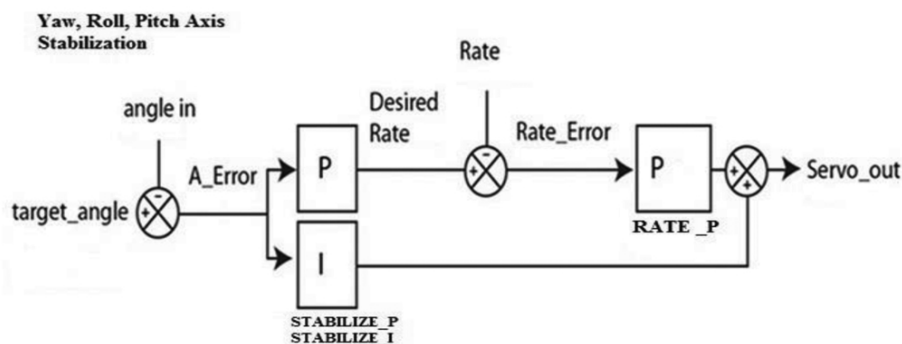


Figure 6. Attitude stabilizer.

The vehicle would be commanded to accelerate depending upon the selected way-point⁷. For instance, if chosen way-indicate is to the right of the vehicle speed vector, then the vehicle will be told to accelerate to right.

In other words, the vehicle will have a tendency to adjust its speed heading to the bearing of L (look-ahead distance). At every single point w.r.t. to the current location of the vehicle, in time a roundabout way can be characterized by the position of the way-point. The acceleration created is equivalent to the centripetal acceleration required to tail this instantaneous circular segment given by $L = 2R\sin\eta$. Therefore, $acc = V^2/R = 2(V^2/L)\sin\eta$.

Subsequently, the lateral acceleration gave by the guidance rationale is suitable to take after a circle of any radius R . This angle fills three needs; it gives a heading deviation angle, for deviations from the craved direction it gives PD control on cross track error and it gives lateral acceleration to precisely take after a roundabout reference trajectory. In case of unavailability of next way-point the PAV would be circling at radius R around the current way-point until the next waypoint is given.

- Parameter: NAV_P is the proportional chosen as 2.2. PAV will fluctuate a bit contingent upon the weight and thrust of the motors.
- Parameter: NAV_D is set to 0 by default.

PI control and PID rate control for altitude hold

The altitude error is figured in centimeters and fed to the controller (Figure 7). The principal phase of the controller takes the altitude error and chooses how quick the PAV ought to go to achieve the correct altitude.

- Parameter: THR_ALT_P is 4 or 4 m/s for a 1 m error. The desired rate maximizes at 1 m/s.
- Parameter: THR_ALT_I is utilized to close the gap between the actual hover throttle and current assumed hover throttle.

Now that we have a desired rate, we need to change the thrust to give us that rate.

- Parameter: THR_RATE_P is the relative reaction and the default is 0.35. PAV will vary quite a bit depending on the weight and thrust of the motors. The worth ought to be brought all together down to minimize the oscillations.
- Parameter: THR_RATE_I is set to 0 as a matter of course.
- Parameter: THR_RATE_D is 0.02 as a matter of course, yet the noise of the Baro sensor can bring issues. If the value is too high awful oscillations are seen.

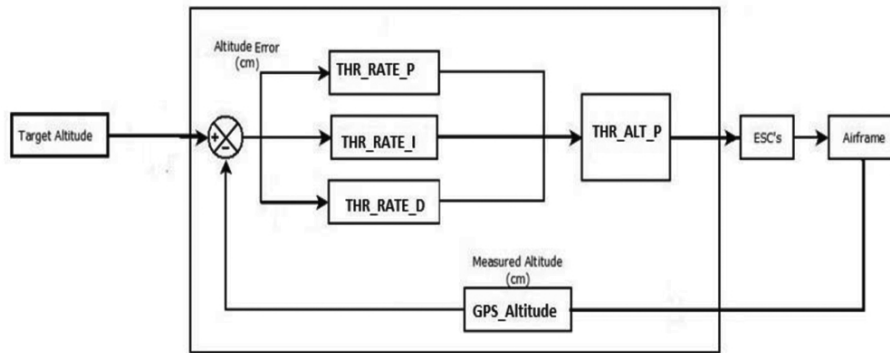


Figure 7. Altitude hold controller.

Table 1. Gain values for theoretical and practical

#	Theoretical ⁸			Practical flight test		
	K _P	K _I	K _D	K _P	K _I	K _D
Attitude	–	–	–	1.3	0	0.0025
Later heading control	1.8	0	0	2.2	0	0
Altitude hold	0.17	0.02	0.01	0.35	0	0.02
	4.5 (Throttle)	–	–	4 (Throttle)	–	–

A similar study⁶ for parafoil vehicle was reported earlier⁸. The theoretical and flight test gains of PAV are compared in Table 1.

Algorithm design for guidance law

The algorithm generally takes in the sensor’s values which are connected to the on-board controller, and a defined path is followed using the sensors data. Using the received sensor information a path is defined for the aerial vehicle. For achieving the defined path the servo motors are controlled automatically to change the direction and BLDC motor is controlled for holding the vehicle at desired altitude. The guidance logic is developed using proportional navigation technique, where the controller gets the latitude, longitude and the altitude values from the GPS and two motors are controlled. The controller then calculates the heading deviation from the way-point and distance to the next waypoint.

Main control loop

The guidance logic is developed using proportional navigation technique (algorithm 1), where the controller gets the latitude, longitude and the altitude values from the GPS. The controller then calculates the heading deviation and distance to the next waypoint and determines whether the vehicle is within the path or not. If it is within the path then the controller executes steer to target algorithm.

If the vehicle deviates from the path due to wind or any other problem then the controller executes path deviation algorithm.

Steer to target algorithm

In this algorithm the vehicle gets the actual heading from the control loop and current heading from GPS and then calculates the heading deviation (algorithm 2). The heading deviation along with gain value is given to the servo with the calculated yaw rate.

Path deviation algorithm

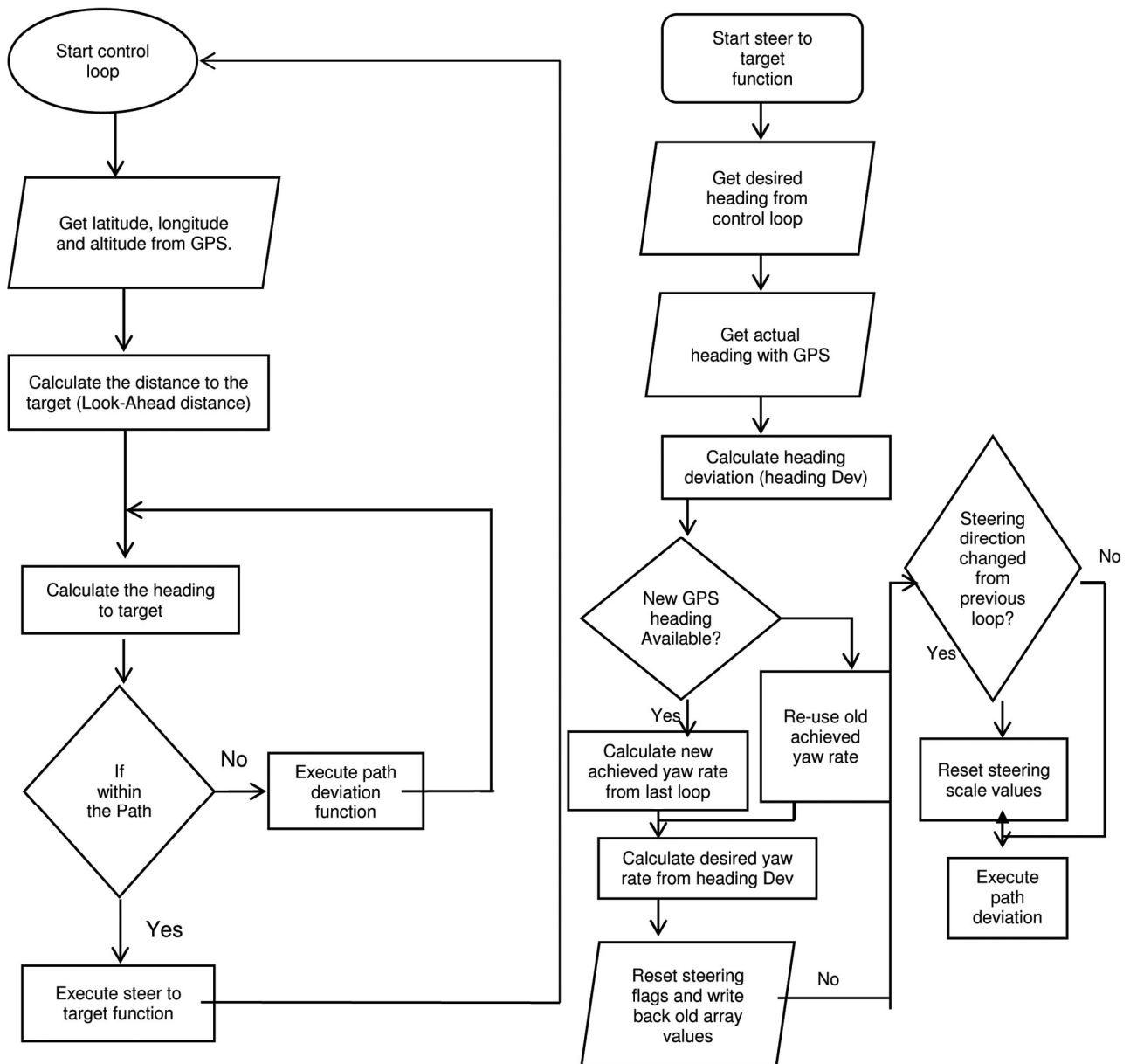
In this algorithm (algorithm 3) the controller compares the heading deviation angle with the desired deviation angle, two conditions occur in the case:

- Heading deviation < desired heading and servo steering angle > 0, then steer servo to left.
- Heading deviation > desired heading and servo steering angle < 0, then steer servo to right.

Flight test results

Stability

The roll and yaw tuning is done and the oscillations are reduced. The theoretical controller tuning parameters are



Algorithm 1. Main control loop.

Algorithm 2. Steer to target algorithm.

incorporated in the micro controller used. The values are further tuned as in practical condition and the wind parameters act on the stability. $K = 1.3$ provides more stability to the system as seen in Figure 8–10.

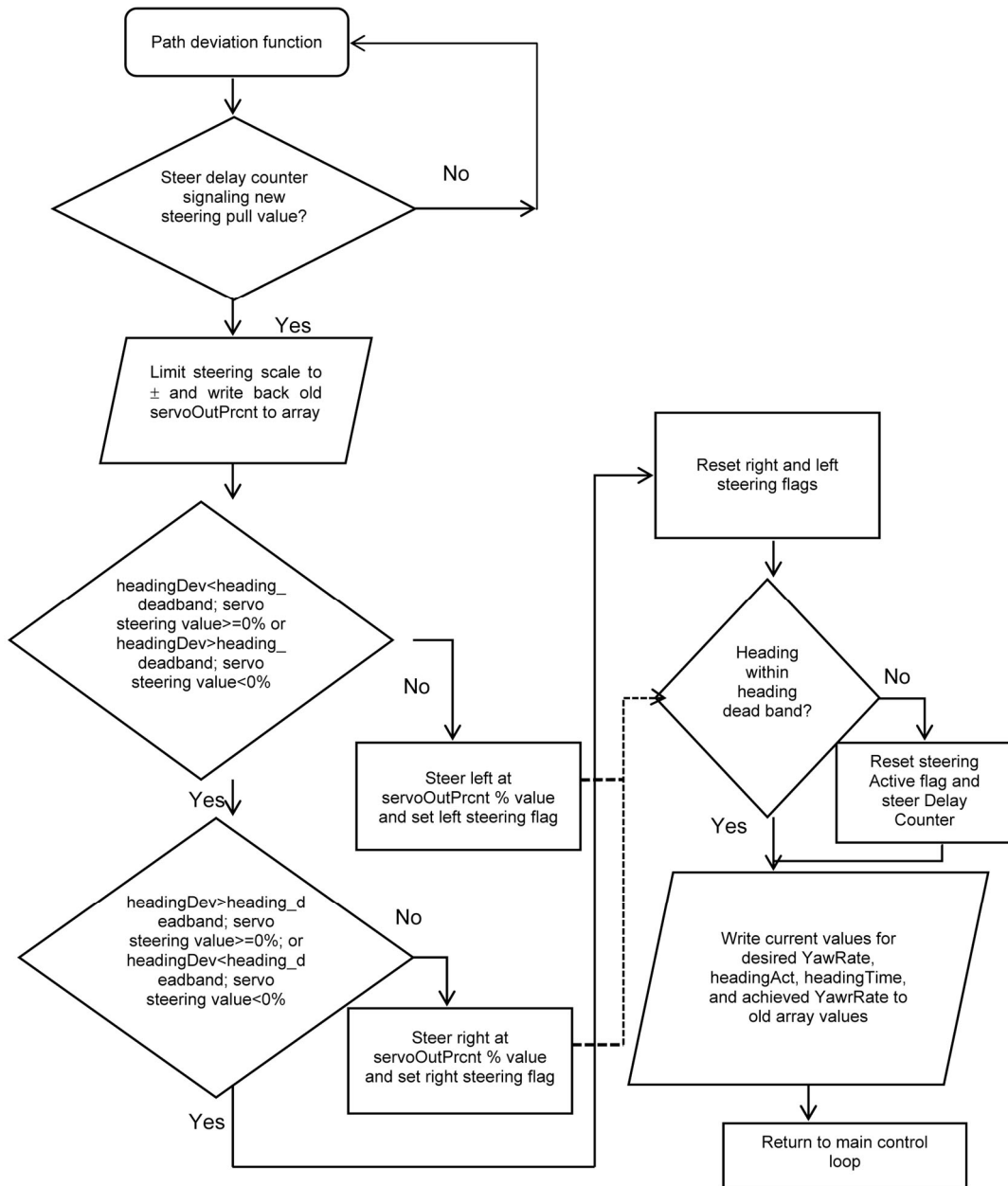
Heading controller

After the attitude stability, lateral heading controller is designed for way-point navigation and loiter operations according to steer to target algorithm. As discussed in the algorithm, the heading deviation goes down to zero as the next waypoint is reached. The lateral tuning parameter $K = 1.8$ implemented in the flight testing showed that

there was further tuning needed due to wind conditions. The practical K tuning implemented is taken as 2.2 for precise steering to the target position. Figure 11 indicates the tilt in servo angle to achieve lateral heading. Figure 12 indicates that in guidance mode, while PAV is travelling from one way point to the other the heading angle reduces to zero. This indicates that the vehicle is approaching the target point.

Longitudinal altitude hold controller

The throttle tuning calculated was 4.5 m/sec, this value was further reduced to 4 m/sec. The PID values remain



Algorithm 3. Path deviation algorithm.

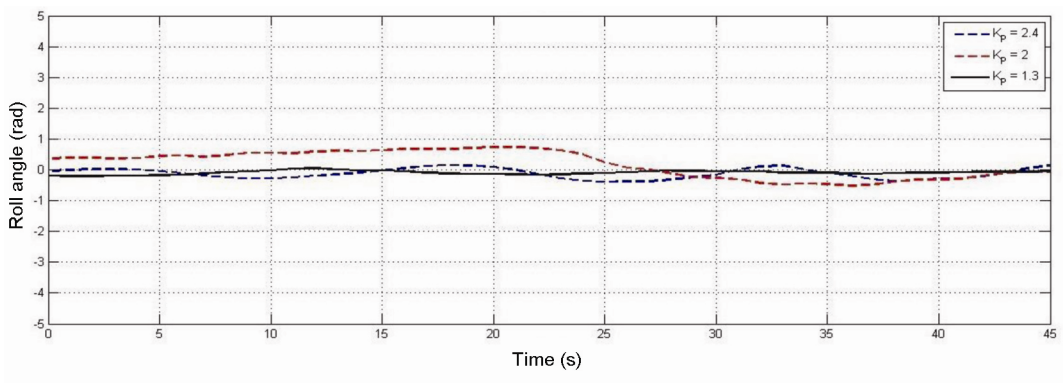


Figure 8. K tuning for roll.

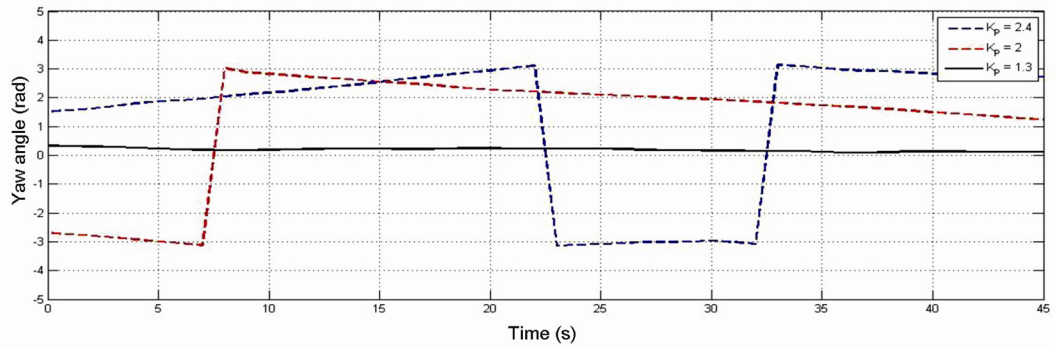


Figure 9. K_p tuning for yaw.

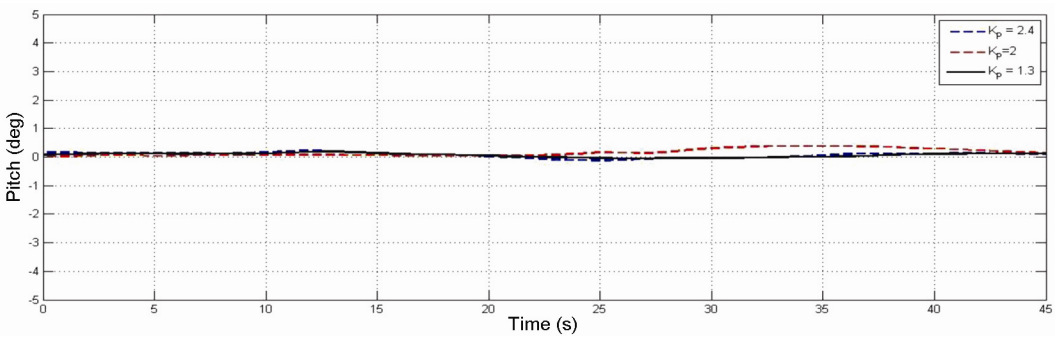


Figure 10. K_p tuning pitch angle.

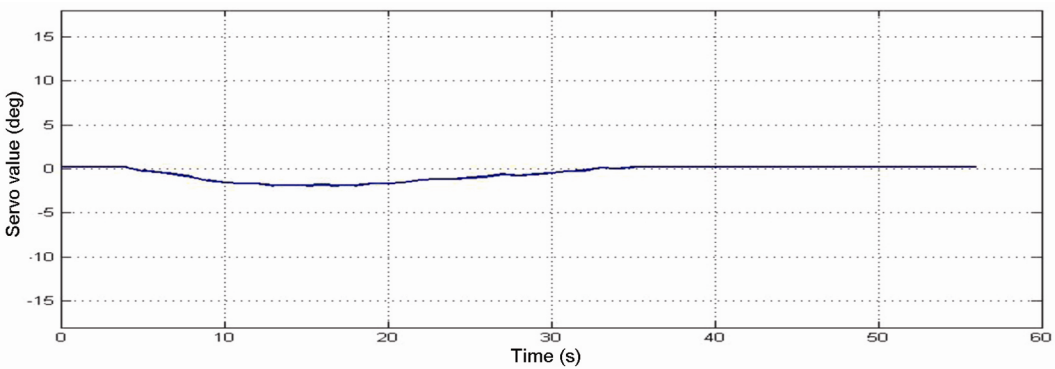


Figure 11. Servo control.

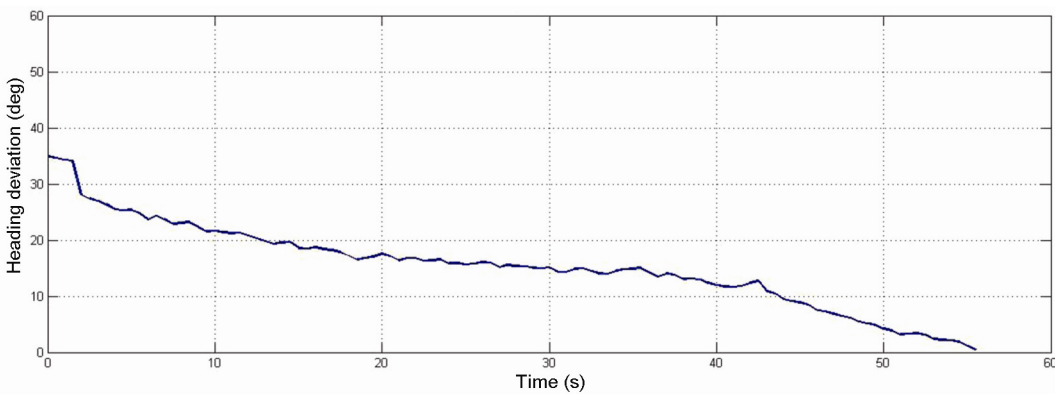


Figure 12. Heading angle.

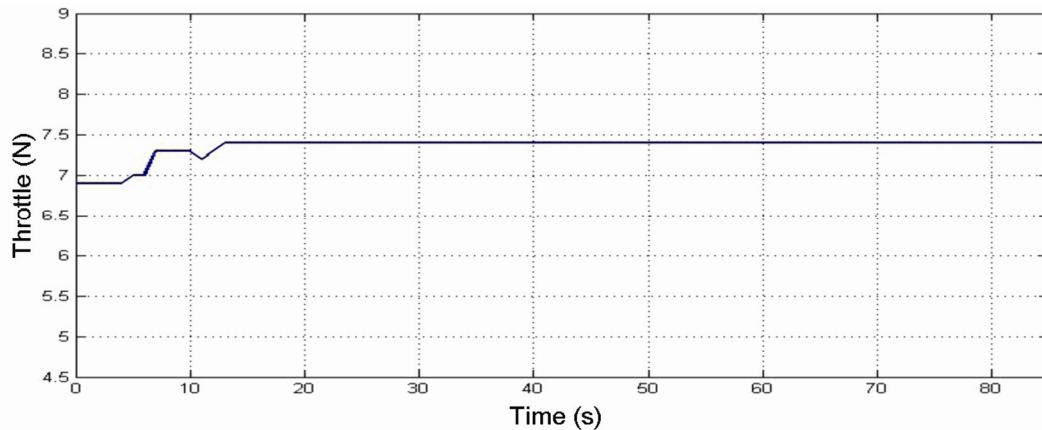


Figure 13. Throttle hold.

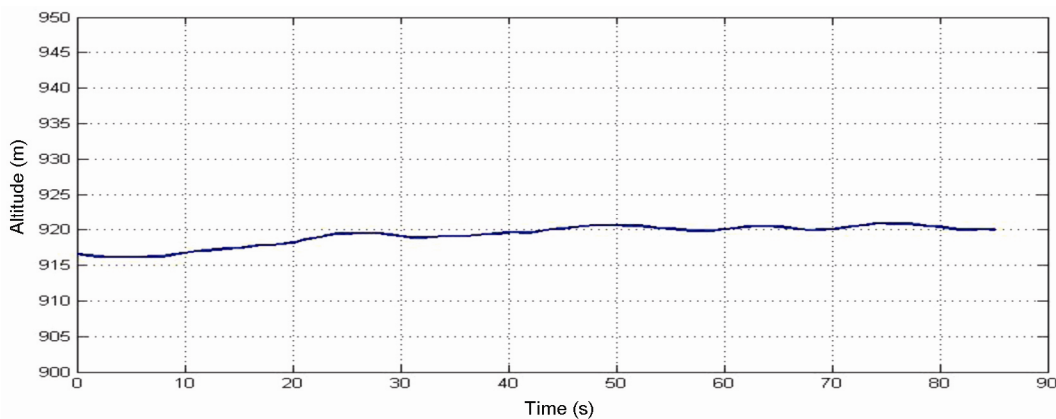


Figure 14. Altitude hold.

the same practically with a small change in K value, which is 0.35 instead of 0.17. Figure 13 indicates that the throttle value is set to 7.5 N holding the altitude at 920 m as shown in Figure 14.

Conclusion and future work

We have provided a comparison of lateral and longitudinal control theoretical results with practical results. The results indicate a small difference, as in flight tests environmental conditions come into picture especially wind conditions. Altitude hold using throttle control was successfully tested in which, stability feedback compensation technique was used. Future work will be directed towards incorporating remote sensing devices such as IR camera with video transmission to the ground station for better data acquisition, which can be used in the applications of oil and gas pipeline monitoring, mining where harmful gases are leaked, aerial surveillance, etc.

1. Lingards, J. S., Precision Aerial Delivery Seminar, Ram-air Parachute Design. 13th AIAA Aerodynamic Decelerator System Technology Conference, Clearwater Beach, May 1995.
2. Devalla, V., Mondal, A. K., Arun Jeya Prakash, A. J. and Prakash, O., Development of position tracking and guidance system for

- Unmanned Powered Parafoil Aerial Vehicle, 4th International Conference on Reliability, Infocom Technologies and Optimization (ICRITO) (Trends and Future Directions), 2015, Noida, 2015, pp. 1–6.
3. Devalla, V and Prakash, O., Developments in Unmanned Powered Parachute Aerial Vehicle: A Review. *IEEE Aerospace Electron. Syst. Soc. Mag.*, November 2014.
4. Prakash, O. and Ananthkrishnan, N., Modeling and simulation of nine degrees of freedom parafoil – payload system flight dynamics, AIAA Atmospheric Flight Mechanics Conference and Exhibit, 21–24 August 2006, Keystone, Colorado.
5. Slegers, N. and Costello, M. Model predictive control of a parafoil and payload system. *J. Guid. Control Dyn.*, 2005, **28**(4), 816–821.
6. Nelson, R. C., *Flight Stability and Automatic Control*, McGraw-Hill, New York, 1989.
7. Park, S., Deyst, J. and How, J. P., A new nonlinear guidance logic for trajectory tracking. Proceedings of the AIAA Guidance, Navigation and Control Conference, August 2004, AIAA-2004-4900.
8. Umenberger, J., Guidance navigation and control of a small-scale paramotor. Proceedings of Australasian Conference on Robotics and Automation, 3–5 December 2012, Victoria University of Wellington, New Zealand.

Received 3 March 2015; revised accepted 5 April 2016

doi: 10.18520/cs/v111/i6/1045-1054